Frustration by competing interactions in the highly distorted double perovskites La_{2}NaB^{′}O_{6} (B^{′}=Ru, Os)

A. A. Aczel, D. E. Bugaris, L. Li, J.-Q. Yan, C. de la Cruz, H.-C. zur Loye, and S. E. Nagler

Phys. Rev. B **87**, 014435 — Published 31 January 2013

DOI: 10.1103/PhysRevB.87.014435

Frustration by competing interactions in the highly-distorted double perovskites $La_2NaB'O_6$ ($B' =$ Ru, Os)

A.A. Aczel,[1,*] D.E. Bugaris,[2] L. Li,[3] J.-Q. Yan,[3,4] C. de la Cruz,[1] H.-C. zur Loye,[2] and S.E. Nagler[1,5]

[1]*Quantum Condensed Matter Division, Neutron Sciences Directorate, Oak Ridge National Laboratory, Oak Ridge, TN 37831, USA*
[2]*Department of Chemistry and Biochemistry, University of South Carolina, Columbia, SC 29208, USA*
[3]*Department of Materials Science and Engineering, University of Tennessee, Knoxville, TN 37996, USA*
[4]*Materials Science and Technology Division, Oak Ridge National Laboratory, Oak Ridge, TN 37831, USA*
[5]*CIRE, University of Tennessee, Knoxville, TN 37996, USA*

(Dated: January 16, 2013)

The usual classical behaviour of $S = 3/2$, B-site ordered double perovskites generally results in simple, commensurate magnetic ground states. In contrast, combined magnetic susceptibility, heat capacity, and neutron powder diffraction measurements for the $S = 3/2$ systems $La_2NaB'O_6$ ($B' =$ Ru, Os) reveal an incommensurate magnetic ground state for La_2NaRuO_6 and a drastically suppressed ordered moment for La_2NaOsO_6. This behaviour is attributed to the large monoclinic structural distortions of these double perovskites. The distortions have the effects of creating inequivalent nearest neighbour (NN) superexchange interactions and weakening them on average, possibly to an energy scale that is comparable with the average next nearest neighbour (NNN) superexchange. The exotic ground states in these materials can then arise from a competition between some combination of inequivalent NN and NNN exchange interactions, providing a novel mechanism for achieving frustration in the double perovskite family.

PACS numbers: 75.30.Fv, 75.40.Cx, 75.47.Lx, 76.30.He

Insulating, B-site ordered double perovskites of the formula $A_2BB'O_6$ have attracted considerable interest recently due to the opportunity to study geometric frustration on a face-centered cubic (FCC) lattice. This situation arises when the only magnetic ions in the system can be associated with the B′ site and are governed by antiferromagnetic (AF) nearest neighbour (NN) interactions. There should also be minimal site mixing between the B and B′ sites. Since the double perovskite structure type is very versatile with respect to chemical substitution and the B sites can accommodate a variety of transition metals, systematic studies can be performed to investigate the effects of changing the spin quantum number S and increasing the relativistic spin-orbit coupling by considering materials with $4d$ and $5d$ electrons. A series of exotic magnetic ground states have been observed previously in $S = 1/2$ and 1 systems, including a collective singlet state coexisting with paramagnetism in Ba_2YMoO_6[1, 2] described as a valence bond glass[3], a collective singlet state in La_2LiReO_6[4], spin freezing without long-range order in Ba_2YReO_6[4], Sr_2MgReO_6[5] and Sr_2CaReO_6[6], short-range order in La_2LiMoO_6[1], and a ferromagnetic (FM) Mott insulating state in Ba_2NaOsO_6[7, 8]. Theoretical studies have also indicated that a wealth of other magnetic ground states are possible in these $4d$ and $5d$ quantum spin systems[9, 10].

$4d$ and $5d$ double perovskites with larger $S = 3/2$ and 5/2 spins are expected to behave more classically. NN AF exchange interactions along extended superexchange B′-O-O-B′ pathways are often dominant in these materials, resulting in Type I AF order, following the notation in Ref. [11]. Since the magnetic atoms are on a geometrically-frustrated FCC lattice, this state is a compromise where eight of the NN spins are AF-aligned, four are FM, and all NNN spins are also FM. There are many examples where this magnetic ground state is realized, including Ca_2LaRuO_6[12], Sr_2YRuO_6[13], Sr_2LuRuO_6, Ba_2YRuO_6, Ba_2LuRuO_6[11], La_2LiRuO_6[14], and Sr_2TeMnO_6[15]. On the other hand, if AF next nearest neighbour (NNN) exchange is the most important interaction, these materials do not show strong frustration effects and are often characterized by Type II AF order[11]. The Type II magnetic state ensures that all NNN spins are AF-aligned. Experimental realizations often consist of non-magnetic W, Nb, Mo or Re on the B site and include Ca_2WMnO_6, Sr_2WMnO_6, Sr_2MoMnO_6[16] and $LaANbCoO_6$ (A = Ca, Ba, Sr)[17]. Finally, Type III AF order has been observed in the system Ba_2LaRuO_6[12]. This state arises when the NN AF interaction is large but the NNN AF interaction is not negligible. While the spin alignment between NNs is the same as for Type I AF, two out of the six NNN spins also become AF in the Type III ordered state.

In the ideal double perovskite cubic structure, both the B and B′ sites form FCC lattices. In practice, many double perovskites exhibit structural distortions from the ideal cubic behaviour, most commonly caused by introducing a very small cation into the A site. This atomic position is indicated by the grey isolated spheres in the double perovskite structure as illustrated in Fig. 1. The structural distortion often lowers the crystal symmetry from cubic to monoclinic. Although the BO_6 and the $B'O_6$ octahedra of these monoclinic double perovskites remain nearly ideal, the structural distortion tilts them by varying degrees, with the amount of tilting depending on both the size of the A site cation and the difference in the ionic radii of the B and B′ sites. The size of the structural distortion is generally quantified by the average tilting of the BO_6 and $B'O_6$ octahedra, defined by $\psi = (180 - \theta)/2$, where θ is the average B-O-B′ angle. Furthermore, the B′ magnetic atoms form a pseudo-FCC sublattice characterized by

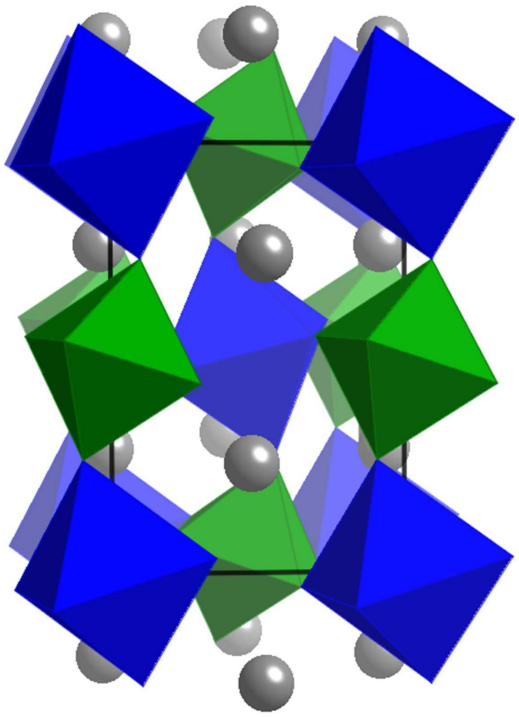

FIG. 1: Double perovskite structure, with the large blue octahedra representing NaO_6, the small green octahedra depicting $(Ru,Os)O_6$, and the isolated grey spheres corresponding to La atoms. The small ionic radius of La leads to a large tilting of the NaO_6 and $(Ru,Os)O_6$ octahedra in La_2NaRuO_6 and La_2NaOsO_6.

two sets each of two-fold degenerate and four-fold degenerate NN distances, with the effect of creating four inequivalent NN exchange interactions. The modified structure has important consequences for the magnetic behaviour. In general, the apparent strength of NN interactions is significantly weaker in distorted systems. Moreover, the geometric frustration in materials where the NN interaction dominates is partially relieved. As typical examples, the cubic system Ba_2YRuO_6 has a Curie-Weiss temperature of -522 K, an ordering temperature of 37 K, and a frustration index of 14, while the same parameters for the monoclinic material La_2LiRuO_6 were found to be -184 K, 23 K, and 8[18].

It is interesting to note that the vast majority of monoclinic double perovskites have β angles that deviate from 90° by less than 0.3°, and so systems with larger monoclinic structural distortions have rarely been studied in detail. One notable exception is the family R_2LiRuO_6, where an additional magnetic sublattice often arises from magnetic rare earth ions R on the A site[19]. In these systems, the Ru atoms generally exhibit Type I AF order while the R atoms form a canted AF arrangement. La_2NaRuO_6 and La_2NaOsO_6 are good candidates for investigating the effects of large monoclinic structural distortions on the magnetic properties of double perovskite systems with magnetic atoms only occupying the B′ sites. Small single crystals of these materials were recently grown by a flux method[20, 21]. The large structural distortions of these systems arise from a small A site cation coupled with a relatively large ionic radii difference between the B and B′ sites. These properties lead to reported β angles of 90.495(2)° and 90.587(2)° and corresponding average octahedral tilts of 17.0° and 17.3° for La_2NaRuO_6 and La_2NaOsO_6 respectively. Recent band structure calculations have been performed and predict that La_2NaRuO_6 is insulating[22]. La_2NaOsO_6 is also expected to be an insulator based on the large spatial separation of the Os ions, and this behaviour has been confirmed in the related system Ba_2NaOsO_6[8].

In this work, we performed magnetic susceptibility, heat capacity and neutron powder diffraction (NPD) measurements to investigate the magnetic ground states of La_2NaRuO_6 and La_2NaOsO_6. Our results reveal a sharp upturn in the magnetic susceptibility and a clear lambda anomaly in the specific heat for La_2NaRuO_6 around T = 15 K, corresponding to an incommensurate magnetic structure with an ordering wavevector of (0 0 1±δ) with $\delta = 0.091$. The magnetic structure is best explained by two independent, interpenetrating helices made up of alternating ab-planes of spins. Surprisingly, despite a similar sharp upturn in the magnetic susceptibility of La_2NaOsO_6 around 12 K, this material exhibits only a broad, weak feature in the specific heat around 10-12 K and no magnetic Bragg peaks are detected down to 4 K. These findings suggests that the ground state consists of only short-range magnetic order or long-range order with a very small moment size. The unconventional magnetic ground states in these materials are attributed to their large structural distortions, caused by some combination of competing inequivalent nearest neighbour and next nearest neighbour extended superexchange interactions.

To obtain several grams of powder for the neutron diffraction measurements, polycrystalline La_2NaRuO_6 was synthesized via a solid state reaction. La_2O_3 (Alfa Aesar, 99.99%) was first activated by heating in air at 1000°C for 12 h, Na_2CO_3 (Mallinckrodt, 99.95%) was dried overnight at 150°C, and RuO_2 was prepared by heating Ru (Engelhard, 99.95%) in air at 1000°C for 24 h. The starting materials were then mixed together in a 1:0.55:1 ratio, and this included a 10% molar excess of Na_2CO_3 to offset the volatilization of Na_2O during heating. This mixture was heated to 500°C in 1 h, held at 500°C for 8 h, heated to 900°C in 1 h, and held at 900°C for 12 h before turning off the furnace and allowing the sample to cool to room temperature. The sample identity was confirmed via powder X-ray diffraction, where the data were collected on a Rigaku Ultima IV powder diffractometer using Cu Kα radiation. Data were collected on the high-speed D/teX Ultra detector in 0.02° steps over the 2θ range 10-80° with a speed of 10°/min.

Polycrystalline La_2NaOsO_6 was also synthesized via a solid state reaction. The starting materials were nearly identical, with the only difference being that Os (J&J Materials Inc.) replaced RuO_2. The heat treatment was also slightly modified, as the starting mixture was heated to 900°C in 1.5 h and held at 900°C for 12 h before turning off the furnace and allowing

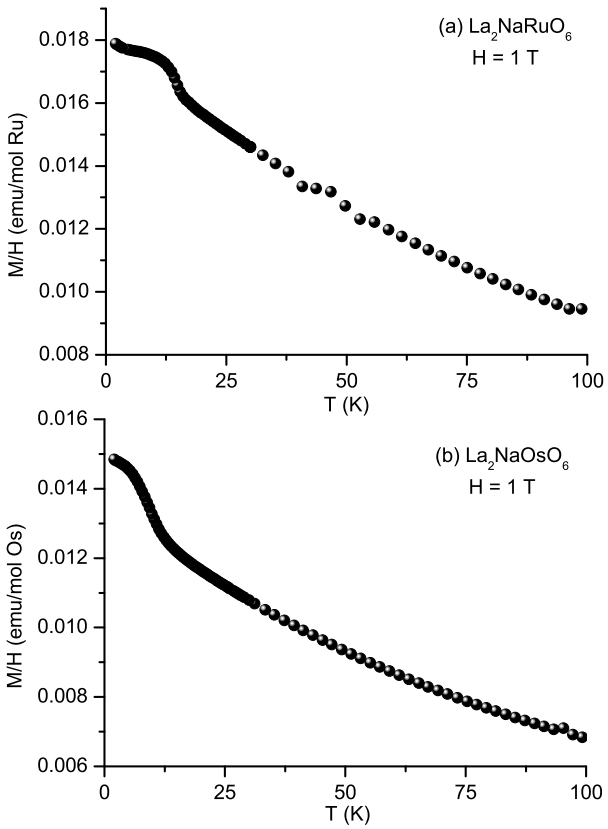

FIG. 2: M/H measurements for (a) La_2NaRuO_6 and (b) La_2NaOsO_6 in an applied field of 1 T and the field-cooled configuration. Both samples exhibit deviations from the Curie-Weiss law at low temperatures, suggesting transitions to magnetically-ordered states.

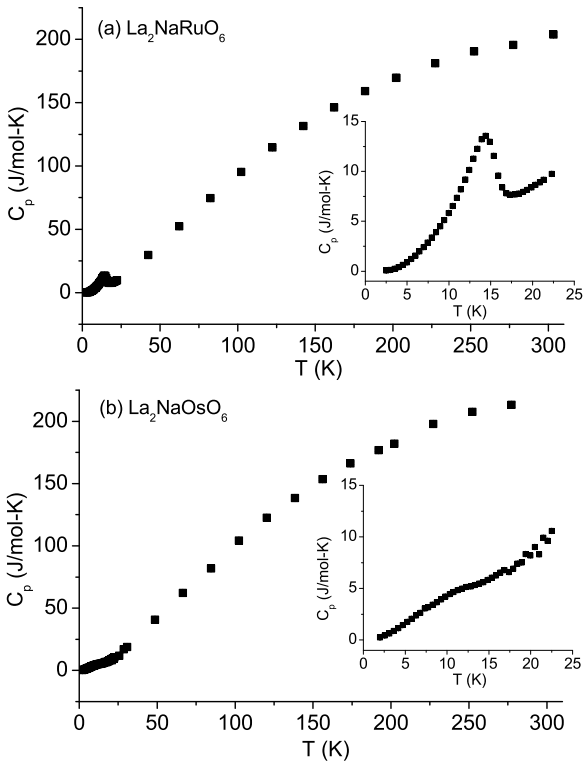

FIG. 3: Heat capacity measurements for (a) La_2NaRuO_6 and (b) La_2NaOsO_6. The insets show the low temperature behaviour for each material. A clear lambda anomaly corresponding to a magnetic transition is visible for La_2NaRuO_6, while only a broad feature is observed in the La_2NaOsO_6 data.

the sample to cool to room temperature. Subsequent powder X-ray diffraction revealed an impurity phase of La_2O_3, so the sample was ground together with additional Na_2CO_3 and Os and then subjected to the same heating profile as before. This step was repeated one additional time, and then powder X-ray diffraction revealed a single phase sample of La_2NaOsO_6.

The heat capacity data was collected in a Physical Property Measurement System and the magnetic susceptibility measurements were obtained from a Magnetic Property Measurement System using cold-pressed pellets. For the NPD experiment, roughly 5 g of each polycrystalline sample was loaded in a closed-cycle refrigerator and studied using the HB-2A powder diffractometer at the High Flux Isotope Reactor of Oak Ridge National Laboratory. Data from HB-2A were collected with neutron wavelengths $\lambda = 1.54$ Å and $\lambda = 2.41$ Å at temperatures of 4 - 300 K using a collimation of $12'$-open-$6'$. The shorter wavelength gives a greater intensity and higher Q coverage that was used to investigate the crystal structures, while the longer wavelength gives lower Q coverage and greater resolution that was important for investigating the magnetic structures of these materials. The NPD data was analyzed using the Rietveld refinement program FullProf[23].

Figure 2 depicts M/H measurements for both La_2NaRuO_6 and La_2NaOsO_6 in an applied field of 1 T. There are significant deviations from Curie-Weiss law behaviour at T $\sim$ 15 K and 12 K for the Ru and Os systems respectively, possibly indicative of magnetic transitions. Fitting the high-temperature data to a Curie-Weiss law in the range 100-300 K yields a Weiss temperature of -57(1) K and an effective moment of 3.43(1) μ_B for La_2NaRuO_6, while a Weiss temperature of -74(1) K and an effective moment of 3.08(1) μ_B was found for La_2NaOsO_6. The field dependence for both materials was also measured at T $= 2$ K and showed no hysteresis. There are some small discrepancies between these results and those obtained on single crystals in Refs. [20, 21]; this may be related to the different ways that the samples were prepared in the two cases and is discussed in more detail below.

The heat capacity measurements for both specimens are presented in Fig. 3 as a function of temperature. The low temperature behaviour is displayed in the insets, and the difference between the two materials is quite striking. The La_2NaRuO_6 data shows a well-defined lambda anomaly around 15 K; this corresponds well to the magnetic transition temperature inferred from the magnetic susceptibility. However, the specific heat of La_2NaOsO_6 is only characterized by a weak, broad feature around 10-12 K, despite a possible

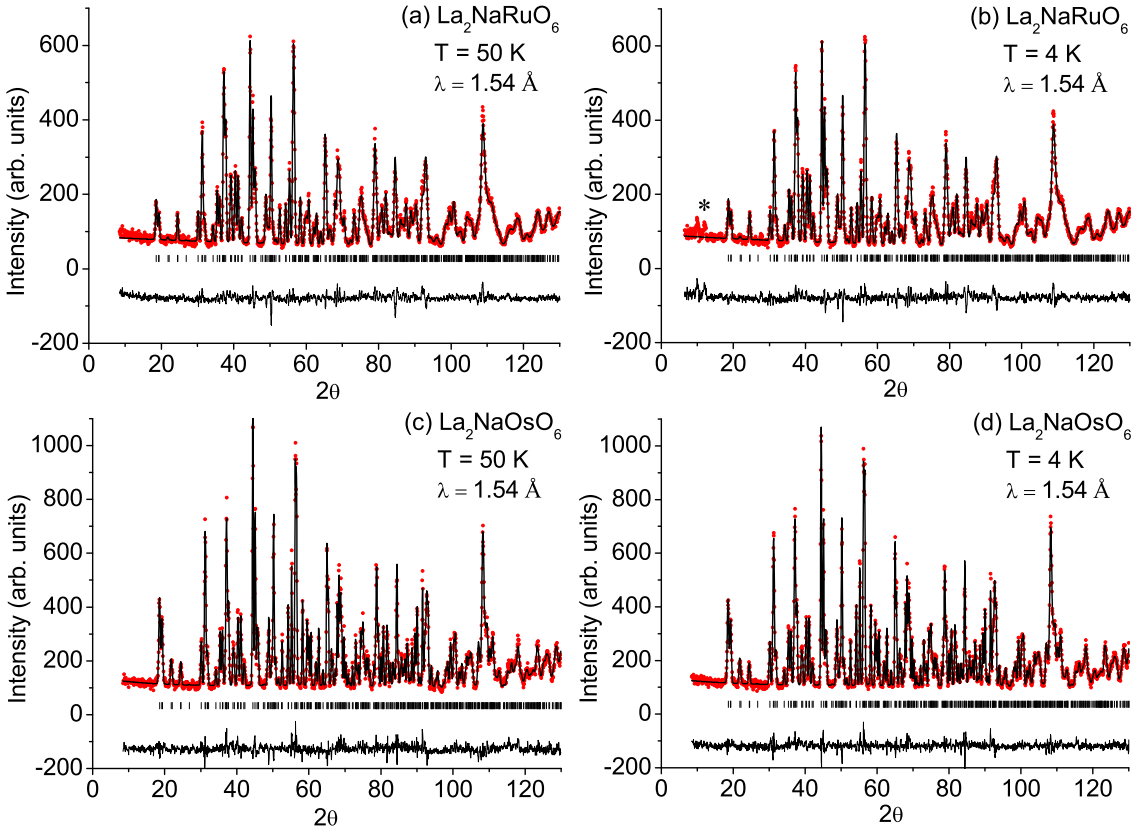

FIG. 4: Neutron diffraction data with $\lambda = 1.54$ Å is shown in (a) and (b) for La_2NaRuO_6 and (c) and (d) for La_2NaOsO_6. The asterisk in (b) labels the largest magnetic Bragg peaks observed in the Ru system at low temperature.

signature of magnetic ordering in the susceptibility measurements observed around the same temperatures.

Figure 4 shows $\lambda = 1.54$ Å NPD data for monoclinic La_2NaRuO_6 and La_2NaOsO_6 at T = 4 K and 50 K, while Table I depicts Rietveld refinement parameters for $\lambda = 1.54$ Å datasets collected at T = 4 K and 300 K. There is no evidence for a structural phase transition between 300 K and 4 K in either material, and the monoclinic structural distortion gradually increases with decreasing temperature. The Rietveld refinements also confirm that there is essentially no site mixing between the Na and Ru/Os atomic positions, as expected for double perovskite systems with a charge difference of +4 between the B and B′ sites[24].

Since La and Na have very similar ionic radii, site mixing between the A and B sites was also included in the refinements and consistently found to be less than 1 %. Moreover, refinements with non-stoichiometric La and Na were considered separately since the materials preparation required excess Na_2CO_3. While no La was found on the B sites, the quality of the refinements for both materials consistently improved when Na was allowed on the A sites, creating a small overall excess of Na and a small deficiency of La in the nominal chemical formulas. The $\lambda = 1.54$ Å datasets collected at T = 4 K, 50 K and 300 K were refined independently for both materials, with the average amount of excess Na on the A sites given by 3(2) % and 10(2) % for La_2NaRuO_6 and La_2NaOsO_6. Flux grown crystals of both materials[20, 21] were not found to contain excess Na, suggesting that there is a small sample dependence related to the way these systems are synthesized. The room-temperature lattice constants for the crystals and polycrystalline samples are not equivalent within one standard deviation, and there are small differences in the magnetic susceptibility of the crystals and powders, both providing additional evidence for this possibility. It is also interesting to note that the room-temperature β angles for polycrystalline La_2NaRuO_6 and La_2NaOsO_6 are smaller than those of their single crystal counterparts. This feature is consistent with some slightly larger ionic radii Na occupying the A sites, and leads to smaller average octahedral tilt values of 16.7° and 16.8° for the polycrystalline Ru and Os systems respectively.

As indicated by the asterisk in Fig. 4(b) and the low angle diffraction plot of the $\lambda = 2.41$ Å data shown in Fig. 5(a), below $\sim$ 16 K additional scattering is observed in the La_2NaRuO_6 neutron diffraction pattern at the incommensurate positions (0 0 1$\pm\delta$). This is indicative of magnetic order with a propagation vector $\vec{k} = (0\ 0\ 0.091)$. Fig. 5(b) shows the temperature-dependence of the (0 0 1-δ) magnetic reflection. The incommensurability was found to be roughly temperature-independent and the transition temperature asso-

ciated with this reflection corresponds well to the the value inferred from susceptibility and heat capacity measurements. To the best of our knowledge, this is the first time that an incommensurate magnetic ground state has been observed in a B-site ordered double perovskite system with only one type of magnetic atom in the unit cell. In fact, incommensurate magnetic ground states are rarely found in double perovskite systems in general. One of the few known examples is the helical spin structure observed in Ba_2CoReO_6[25], a material with two types of magnetic atoms.

TABLE I: Structural parameters for La_2NaRuO_6 and La_2NaOsO_6 at T = 4 K and T = 300 K extracted from the refinements of the $\lambda = 1.54$ Å neutron powder diffraction data.

(a) La_2NaRuO_6
Space group $P2_1/n$

Lattice parameters and refinement quality		
T	4 K	300 K
a	5.5878(1) Å	5.6084(2) Å
b	5.9016(1) Å	5.9107 (2) Å
c	7.9902(2) Å	8.0190(3) Å
β	90.387(2)°	90.348(3)°
χ^2	3.07	3.58
R_{wp}	6.33 %	6.77 %

Atom positions at T = 4 K				
Atom	Site	x	y	z
La	4e	0.4840(4)	0.0643(2)	0.2523(3)
Na	2a	0	0	0
Ru	2b	0.5	0.5	0
O_1	4e	0.2109(5)	0.3230(5)	0.0477(4)
O_2	4e	0.6016(5)	0.4637(5)	0.2319(4)
O_3	4e	0.3281(6)	0.7798(5)	0.0571(4)

(b) La_2NaOsO_6
Space group $P2_1/n$

Lattice parameters and refinement quality		
T	4 K	300 K
a	5.6062(1) Å	5.6284(1) Å
b	5.9173(1) Å	5.9248(1) Å
c	8.0297(1) Å	8.0603(2) Å
β	90.457(1)°	90.413(2)°
χ^2	2.80	4.34
R_{wp}	5.60 %	6.00 %

Atom positions at T = 4 K				
Atom	Site	x	y	z
La	4e	0.4844(3)	0.0623(2)	0.2523(3)
Na	2a	0	0	0
Os	2b	0.5	0.5	0
O_1	4e	0.2129(4)	0.3245(4)	0.0471(3)
O_2	4e	0.6023(4)	0.4609(4)	0.2299(3)
O_3	4e	0.3314(4)	0.7784(4)	0.0588(3)

As shown in Fig. 6(a), the (001) magnetic satellites of La_2NaRuO_6 are very intense relative to other magnetic peaks, including the overlapping (010) satellites centered around $2\theta = 23.6°$ and the overlapping (100) satellites centered

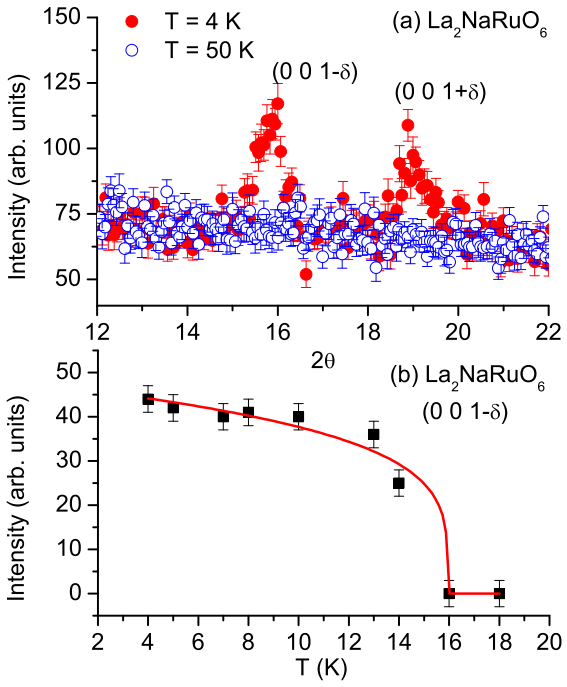

FIG. 5: (a) $\lambda = 2.41$ Å NPD data showing the (0 0 1$\pm\delta$) magnetic peaks that appear at low temperature. (b) Intensity of the incommensurate (0 0 1-δ) peak plotted as a function of temperature, indicating a magnetic transition at T = 16 K in good agreement with magnetic susceptibility and heat capacity data. The solid curve is a guide to the eye.

around $2\theta = 24.9°$, suggesting that the ordered spins align in the ab-plane. The simplest incommensurate magnetic structures consistent with this feature and the observed propagation vector are single helical and sinusoidal spin density wave arrangements. However, these spin configurations yield very little intensity for the satellite peaks around the (001) Bragg position and are instead characterized by strong (002) satellite peaks; both of these features are clearly inconsistent with the data. Refinements based on models assuming simple conical and cycloidal magnetic structures, allowing for spin components along the c-axis, were also tested as a consistency check, but failed to explain the data.

For these reasons, incommensurate magnetic structures were considered that consist of two independent, interpenetrating helices, with every other ab-plane of spins forming a single helix characterized by a turn angle of $\sim 32.7°$. The refinement result using the $\lambda = 2.41$ Å data and a model assuming that the helices have the same chirality is shown in Fig. 6(a); this magnetic structure reproduces the intensity for the (001) satellite reflections very well. One can also obtain good agreement with the data by using a similar model where the two helices have opposite chirality instead. These two magnetic structures are depicted in Fig. 6(b) and (c), with the alternating colors representing the planes forming the two different helices. In both cases, the ordered moment size for Ru was found to be 1.87(7) μ_B. Although the magnitude of

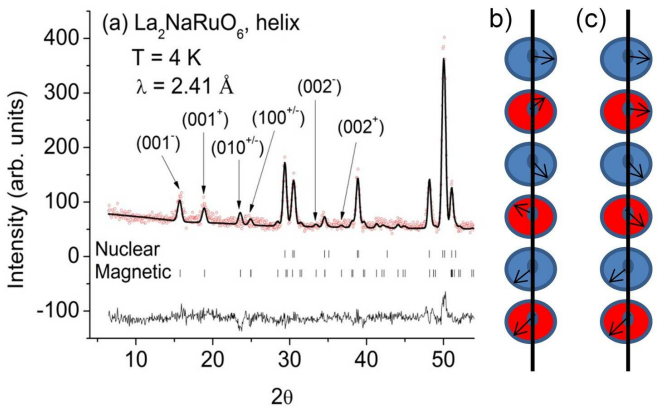

FIG. 6: (a) La_2NaRuO_6 Rietveld refinement results with $\lambda = 2.41$ Å for a magnetic model of two independent, interpenetrating helices. Some selected magnetic Bragg peak positions are labelled. (b), (c) Two possible helical magnetic structures discussed in the text, with the different colors corresponding to the ab-planes that make up the two helices. Although (c) is shown with no relative phase angle between the helices, this is only for simplicity and is not strictly true. The refinement actually yielded a relative phase angle of 104(5)°.

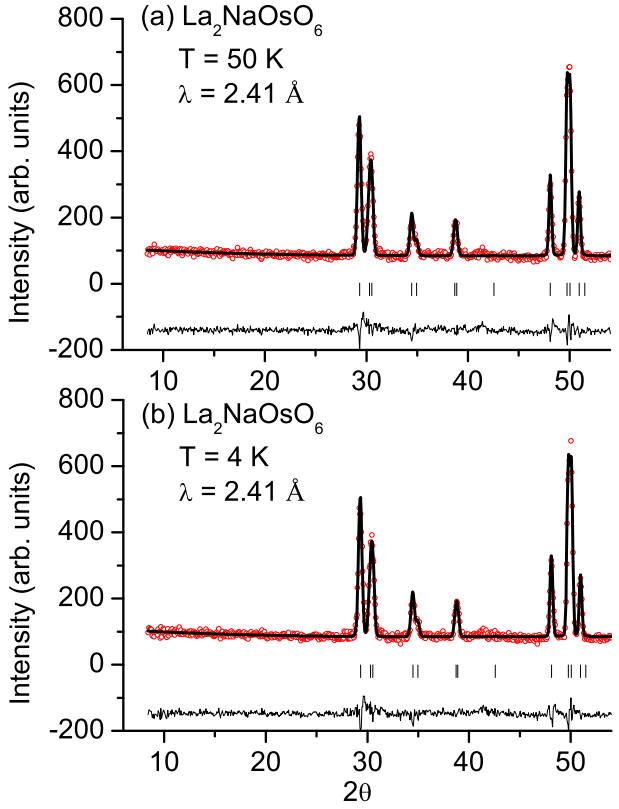

FIG. 7: La_2NaOsO_6 neutron diffraction data with $\lambda = 2.41$ Å, indicating the absence of magnetic peaks down to 4 K.

the Ru moment from the refinements is much smaller than the spin-only value of 3 μ_B, the former is consistent with the ordered moments reported for other Ru double perovskites (see e.g. [12, 13]). Since the Ru^{5+} magnetic form factor is not available in the literature, the refinements were attempted with the $< j_0 >$ form factors for both Ru^{+} and Os^{5+}[26] and the results yielded the same ordered moment sizes for Ru within one standard deviation. Note that magnetic models consisting of two interpenetrating spin density waves can also be used to describe the data, although these spin configurations are rare in insulating magnets.

As shown in Fig. 7, no additional scattering is observed in the La_2NaOsO_6 neutron diffraction pattern down to 4 K despite the relatively large Os^{5+} spin $S = 3/2$ and a possible signature of magnetic ordering in the susceptibility data. A rough upper limit of 0.2 μ_B was determined for the Os ordered moments associated with a series of possible commensurate antiferromagnetic ground states by performing trial refinements. More specifically, if the Os moment size was fixed to be greater than 0.2 μ_B in these models, the simulations consistently produced magnetic Bragg peaks that were not observed in the experimental data with intensities larger than the background noise.

There are several factors that can explain the decrease of the Os moment from the spin-only value, and they are often applicable to 4d magnetic systems such as La_2NaRuO_6 also. Increased covalency causing delocalization of the magnetic moments, arising from greater orbital overlap between spatially-extended 4d and 5d orbitals and neighbouring anion p orbitals, is one possibility that should be taken into consideration. For example, the OsO_6 octahedra of the related double perovskite system Ba_2NaOsO_6 likely form molecular orbitals due to the comparable energy scales of the Os 5d and O 2p orbitals[8]. Spin-orbit coupling plays an important role in the magnetism of 4d, and especially 5d, systems also[27], and is another mechanism that can lead to a reduction in the spin-only value of the ordered moment. Finally, the magnetic Bragg peaks of 4d and 5d systems tend to be weaker than for their 3d counterparts due to the 4d and 5d magnetic form factors decreasing at a faster rate with increasing Q.

To appreciate the magnitude of these different effects on an Os^{5+} material, it is instructive to consider the systems $NaOsO_3$ and Ca_3LiOsO_6. A combined neutron and X-ray study for $NaOsO_3$[28] revealed an Os ordered moment of 1.0(1) μ_B, while the magnetic structure of Ca_3LiOsO_6 was also determined recently[29] and found to have an ordered Os moment of 2 - 2.3 μ_B. The local environment of the magnetic atoms in these two materials is very similar to La_2NaOsO_6. In all three cases, the Os atoms are in slightly-distorted octahedral oxygen cages with nearly identical Os-O bond lengths and no O-Os-O angle deviating from 180° or 90° by more than 1°, so any covalency effects that reduce the ordered Os moment in these materials should not be drastically different. Due to the orbital singlet ground states of the Os atoms in these systems, spin-orbit coupling should also have a negligible effect on reducing the ordered moment size. Moreover, the expected antiferromagnetic ground state for La_2NaOsO_6 should produce some strong magnetic peaks below the (002)

Bragg position. This regime corresponds to Q values of ~ 1.5 Å^{-1} or less and is characterized by a magnetic form factor for Os^{5+} that is $> 80\%$[26] of the $Q = 0$ value. This discussion clearly shows that these three effects are not completely responsible for the very small ordered moment size or absence of long-range magnetic ordering in La_2NaOsO_6, and therefore an additional factor also contributes to this behaviour.

La_2NaRuO_6 and La_2NaOsO_6 are not characterized by conventional Type I or Type II AF long-range order, and therefore possess very unusual magnetic properties for insulating, S = 3/2, B-site ordered double perovskite systems with magnetic atoms only occupying the B′ sites. While the incommensurate magnetic structure of the Ru system and the large reduction in the ordered moment of both materials are typical features of geometrically-frustrated systems, the origin of the unconventional magnetism is initially puzzling when one considers that the large structural distortions should relieve some of the frustration inherent to a perfect FCC magnetic sublattice. However, these same structural distortions can also have a large impact on the strength and sign of the NN and NNN extended superexchange interactions via the tilting of the $B'O_6$ and the BO_6 octahdera. This tilting leads to a series of inequivalent NN and NNN exchange interactions with an average reduced strength, and there are known cases for double perovskites where large monoclinic distortions have led to deviations from typical Type I and Type II AF order.

One prominent example is outlined in Ref. [30], where Sr_2SbCrO_6 is characterized by a Type I AF ground state, while the more highly-distorted system Ca_2SbCrO_6 is ferromagnetic. The large tilting of the $B'O_6$ and BO_6 octahedra in Ca_2SbCrO_6 presumably result in some or all of the inequivalent NN superexchange paths becoming ferromagnetic, leading to the observed ground state. With this in mind, the most likely scenario that explains the unconventional magnetism in La_2NaRuO_6 and La_2NaOsO_6 should be based on finely-tuned, competing, extended superexchange interactions. The competition may be driven by inequivalent FM and AFM NN exchange interactions, or by AF NN and NNN interactions of similar strength. Note that combined AF NN and FM NNN interactions cannot be responsible for the unconventional magnetism observed in these materials, as this situation should result in Type I AF. The best way to definitively determine the origin of the competing magnetic interactions for these two materials is by performing an inelastic neutron scattering study on single crystals. Furthermore, detailed theoretical investigations of the extended superexchange interactions may help to provide additional insight explaining why these systems are characterized by different magnetic ground states. Since the magnitude of the structural distortions in the two materials is very similar, the different radial extent of the Ru $4d$ and Os $5d$ orbitals seems to play an important role in the magnetic properties of these systems. Another possible, although more unlikely, scenario is that the small difference in the amount of excess Na in the two samples may also influence the magnetic ground states by having a direct effect on the NNN extended superexchange paths.

In conclusion, we have investigated the magnetic properties of the highly-distorted double perovskites La_2NaRuO_6 and La_2NaOsO_6 via magnetic susceptibility, heat capacity and neutron powder diffraction. In contast to the Type I and II AF order most commonly found for $S = 3/2$ and 5/2 double perovskite systems, our neutron diffraction results reveal an incommensurate magnetic ground state for La_2NaRuO_6 with a propagation vector of (0 0 0.091). Moreover, despite a possible signature of magnetic ordering from magnetic susceptibility measurements, only a broad, weak feature is observed in the specific heat and no magnetic Bragg peaks are detected for La_2NaOsO_6. The unconventional magnetism of these materials is best explained by some combination of competing, inequivalent NN and NNN extended superexchange interactions, arising from the large monoclinic structural distortions.

We acknowledge V.O. Garlea and J.E. Greedan for useful discussions. This research was supported by the US Department of Energy, Office of Basic Energy Sciences. A.A.A., C.d.l.C. and S.E.N. were supported by the Scientific User Facilities Division, and J.-Q.Y. was supported by the Materials Science and Engineering Division. The neutron experiments were performed at the High Flux Isotope Reactor, which is sponsored by the Scientific User Facilities Division. D.E.B. and H.z.L. would like to acknowledge financial support through the Heterogeneous Functional Materials for Energy Systems (HeteroFoaM) Energy Frontiers Research Center (EFRC), funded by the US Department of Energy, Office of Basic Energy Sciences under award number DE-SC0001061.

* author to whom correspondences should be addressed: E-mail:[aczelaa@ornl.gov]

[1] T. Aharen, J.E. Greedan, C.A. Bridges, A.A. Aczel, J. Rodriguez, G.J. MacDougall, G.M. Luke, T. Imai, V.K. Michaelis, S. Kroeker, H.D. Zhou, C.R. Wiebe and L.M.D. Cranswick, Phys. Rev. B **81**, 224409 (2010).

[2] J.P. Carlo, J.P. Clancy, T. Aharen, Z. Yamani, J.P.C. Ruff, J.J. Wagman, G.J. Van Gastel, H.M.L. Noad, G.E. Granroth, J.E. Greedan, H.A. Dabkowska and B.D. Gaulin, Phys. Rev. B **84**, 100404(R), (2011).

[3] M.A. de Vries, A.C. Mclaughlin and J.W.G. Bos, Phys. Rev. Lett. **104**, 177202 (2010).

[4] T. Aharen, J.E. Greedan, C.A. Bridges, A.A. Aczel, J. Rodriguez, G.J. MacDougall, G.M. Luke, V.K. Michaelis, S. Kroeker, C.R. Wiebe, H.D. Zhou and L.M.D. Cranswick, Phys. Rev. B **81**, 064436 (2010).

[5] C.R. Wiebe, J.E. Greedan, P.P. Kyriakou, G.M. Luke, J.S. Gardner, A. Fukaya, I.M. Gat-Malureanu, P.L. Russo, A.T. Savici and Y.J. Uemura, Phys. Rev. B **68**, 134410 (2003).

[6] C.R. Wiebe, J.E. Greedan, G.M. Luke and J.S. Gardner, Phys. Rev. B **65**, 144413 (2002).

[7] K.E. Stitzer, M.D. Smith and H.-C. zur Loye, Solid State Science **4**, 311 (2002).

[8] A.S. Erickson, S. Misra, G.J. Miller, R.R. Gupta, Z. Schlesinger, W.A. Harrison, J.M. Kim and I.R. Fisher, Phys. Rev. Lett. **99**, 016404 (2007).

[9] G. Chen, R. Pereira and L. Balents, Phys. Rev. B **82**, 174440 (2010).

[10] G. Chen and L. Balents, Phys. Rev. B **84**, 094420 (2011).

[11] P.D. Battle and C.W. Jones, Journal of Solid State Chemistry **78**, 108 (1989).

[12] P.D. Battle, J.B. Goodenough and R. Price, Journal of Solid State Chemistry **46**, 234 (1983).

[13] P.D. Battle and W.J. Macklin, Journal of Solid State Chemistry **52**, 138 (1984).

[14] P.D. Battle, C.P. Grey, M. Hervieu, C. Martin, C.A. Moore and Y. Paik, Journal of Solid State Chemistry **175**, 20 (2003).

[15] L. Ortega-San Martin, J.P. Chapman, L. Lezama, J.S. Marcos, J. Rodriguez-Fernandez, M.I. Arriortua and T. Rojo, Eur. J. Inorg. Chem. 1362 (2006).

[16] A. Munoz, J.A. Alonso, M.T. Casais, M.J. Martinez-Lope and M.T. Fernandez-Diaz, J. Phys. Cond. Matt. **14**, 8817 (2002).

[17] J.W.G. Bos and J.P. Attfield, Phys. Rev. B **70**, 174434 (2004).

[18] T. Aharen, J.E. Greedan, F.L. Ning, T. Imai, V.K. Michaelis, S. Kroeker, H.D. Zhou, C.R. Wiebe and L.M.D. Cranswick, Phys. Rev. B **80**, 134423 (2009).

[19] S.J. Makowski, J.A. Rodgers, P.F. Henry, J.P. Attfield and J.W.G. Bos, Chem. Mater. **21**, 264 (2009).

[20] W.R. Gemmill, M.D. Smith and H.-C. zur Loye, Journal of Solid State Chemistry **177**, 3560 (2004).

[21] W.R. Gemmill, M.D. Smith, R. Prozorov and H.-C. zur Loye, Inorg. Chem. **44**, 2639 (2005).

[22] A.S. Ahmed, H. Chen and H.K. Yuan, Phys. Stat. Sol. **245**, 720 (2008).

[23] J. Rodriguez-Carvajal, Physica B **192**, 55 (1993).

[24] M. T. Anderson, K. B. Greenwood, G. A. Taylor and K. R. Poppelmeier, Prog. Solid State Chem. **22**, 197 (1993).

[25] C.P. Khattak, C.E. Cox and F.F.Y. Wang, AIP Conf. Proc. **10** 674 (1973).

[26] K. Kobayashi, T. Nagao and M. Ito, Acta Cryst. **A67**, 473 (2011).

[27] B.J. Kim, H. Jin, S.J. Moon, J.Y. Kim, B.G. Park, C.S. Leem, J. Yu, T.W. Noh, C. Kim, S.J. Oh, J.H. Park, V. Durairaj, G. Cao and E. Rotenberg, Phys. Rev. Lett. **101**, 076402 (2008).

[28] S. Calder, V.O. Garlea, D.F. McMorrow, M.D. Lumsden, M.B. Stone, J.C. Lang, J.-W. Kim, J.A. Schlueter, Y.G. Shi, K. Yamaura, Y.S. Sun, Y. Tsujimoto and A.D. Christianson, Phys. Rev. Lett. **108**, 257209 (2012).

[29] S. Calder, M.D. Lumsden, V.O. Garlea, J.-W. Kim, Y.G. Shi, H.L. Feng, K. Yamaura and A.D. Christianson, Phys. Rev. B **86**, 054403 (2012).

[30] M. Retuerto, M. Garcia-Hernandez, M.J. Martinez-Lope, M.T. Fernandez-Diaz, J.P. Attfield and J.A. Alonso, Journal of Materials Chemistry **17**, 3555 (2007).